

# Statistical Estimation of Turbulent Trailing Edge Noise

C.J. Doolan, C. Albarracin Gonzalez and C. H. Hansen

School of Mechanical Engineering, University of Adelaide, Adelaide, Australia

PACS: 43.28.Ra

## ABSTRACT

A new computational aeroacoustic model suitable for the prediction of turbulent airfoil trailing edge noise is presented. The method (known as the RANS based Statistical Noise Model or RSNM) combines numerically generated, mean turbulence information with a Green's function for a semi-infinite half-plane to generate a far-field acoustic auto-spectrum. As a preliminary application of the method, the acoustic spectrum created by turbulent flow past the sharp trailing edge of a flat plate at a Reynolds number ( $Re$ ) of  $5.5 \times 10^5$  is calculated. Four different turbulence models are used to provide the required mean flow data which is used with RSNM. The predicted spectra are shown to agree well with a semi-empirical model from the literature.

## INTRODUCTION

The efficient computation of airfoil trailing edge noise is important for the cost-effective design of fixed and rotary-wing aircraft, wind turbines, fans and submarines. Airfoil self noise occurs when an airfoil shape is placed in an otherwise uniform and steady fluid flow. As in most aeroacoustic noise generation situations, noise is generated by flow unsteadiness. In the case of airfoil self noise, it is the interaction of flow unsteadiness (usually in the form of fluid turbulence) with the surfaces of the airfoil that generates sound. In this paper, we are concerned with the creation of sound by the interaction of flow unsteadiness (turbulence) with a sharp trailing edge. In acoustic terms, the edge presents itself as a sharp impedance discontinuity. This discontinuity scatters acoustic waves generated by fluid turbulence and creates an intensified radiated acoustic field. More detailed descriptions of the trailing edge noise generation processes can be found in Blake (1986) and theoretical descriptions of acoustic scattering and diffraction mechanisms can be found in Morse and Ingard (1986).

Recently, the computation of trailing edge noise has mainly been attempted using either direct or hybrid methods of computational aeroacoustics (CAA). In the direct method, both the fluid dynamics and acoustics are computed in a single step. Recent approaches either use direct numerical simulation (DNS) (Sandberg and Sandham 2008) or large eddy simulation (LES) (Gloerfelt and Garrec 2009) to compute the unsteady compressible flow along with the subsequent acoustic waves in the far-field. While successful, these methods require computational resources of a scale that render them not very suitable for engineering design. To overcome some of these difficulties, hybrid methods have been developed. Hybrid methods use an analytical acoustic analogy to compute the acoustic properties in the far-field using source terms obtained from an unsteady flow calculation. Typically, LES is used to calculate the source terms. This is more efficient than a direct computation as a fine mesh is only required in areas where viscous effects are important. Some recent examples of hybrid CAA for turbulent trailing edge noise include Marsden et al. (2007), Manoha et al. (2000) and Winkler et al. (2009).

As with direct methods, hybrid techniques give accurate results however, the time taken to compute the necessary unsteady

LES data is large and makes their use in engineering design cumbersome. At present and for the near to medium term, it is expected that solving of the steady Reynolds Averaged Navier Stokes (RANS) equations will be the computational design method of choice, due to its relatively modest computational requirements. Unfortunately, RANS solutions are time averaged, and therefore most of the information required to construct the acoustic source terms is missing. Therefore to use RANS solutions for the computation of trailing edge noise, additional modelling of the turbulent flow spectrum is needed. Even with this additional modelling requirement, using a RANS solution to calculate noise will have the benefits of decreasing design and development time as well as improving the performance of numerical optimisation schemes.

Despite its importance, there have only been a few previous attempts at using RANS solutions to calculate turbulent trailing edge noise. Most previous attempts to calculate far-field acoustic pressure rely upon estimating the surface pressure spectrum. Lutz et al. (2007) and Kamruzzaman et al. (2008) use RANS solutions to generate a wall pressure spectrum at the trailing edge of an airfoil. This spectrum is then converted to a far-field acoustic spectrum using a diffraction analogy technique (Chandiramani 1974). The method predicts the correct spectral shape but has difficulty, at present, in obtaining the correct pressure levels. Glegg et al. (2008) used the findings of Spitz (2005) to develop another RANS based trailing edge noise prediction technique. Here, a four dimensional model of the vorticity field is used to estimate the surface pressure spectrum. The turbulent kinetic energy in the boundary layer is obtained from a RANS calculation and used to calculate a mean square vortex sheet strength, that is in-turn used to calculate the amplitude of the wall pressure spectrum. This method has been shown to be successful in calculating trailing edge noise spectra.

A limitation of the above-mentioned methods is that they assume the turbulence field is homogeneous in the streamwise and spanwise directions. This may not be the case in many trailing edge configurations, or in the case where spanwise modifications such as serrations are used. Therefore, a more general technique is desirable, that can relate the flow properties in any region of the boundary layer to the far-field noise.

Another RANS based technique for calculating trailing edge

noise has been developed by Ewert (2008), Ewert et al. (2009). Here, a stochastic method is used to generate time-based turbulence data about the trailing edge, using a RANS simulation as input. The time based data are then used with a numerical CAA calculation to generate the far-field noise spectrum. The advantage of this method is that it is general so it can be used for a wide variety of problems and is not limited to trailing edge noise. The disadvantage is that it has numerical requirements that are of the same order or larger than the RANS calculation used to generate the stochastic signals. Jones et al. (2010) have suggested a method for reducing computational time by replacing the numerical acoustic calculation with an acoustic analogy approach.

This paper will describe a new method of calculating turbulent trailing edge noise using RANS calculated turbulence data, known as the RANS based Statistical Noise Method or RSNM. This method differs from others in that it does not attempt to estimate a surface pressure spectrum or numerically propagate stochastically generated noise. Instead, the method uses a Green's function for a semi-infinite half-plane to generate a far-field acoustic auto-spectrum directly using a statistical model for the turbulence in the boundary layer about the trailing edge. A turbulent velocity cross-spectrum model must be assumed in order for the method to be successful. The choice of this model must accurately reflect the frequency and phase distribution in the boundary layer. The development of this model was inspired by the recent work of Tam and Auriault (1999) and Morris and Farassat (2002) who developed useful models of jet noise that use RANS data to assemble the source terms.

As a preliminary application of this method, the acoustic spectrum generated by turbulent flow past the sharp trailing edge of a flat plate at a Reynolds number ( $Re$ ) of  $5.5 \times 10^5$  is calculated. A flat plate is chosen as it is the simplest trailing edge configuration where the boundary layer is approximately homogeneous in the spanwise and streamwise directions, therefore allowing comparison with existing trailing edge noise theories that use semi-empirical surface pressure spectrum models.

## SUMMARY OF THE NOISE PREDICTION METHOD

This section will summarise the noise prediction methodology. Only the final derived equations are presented here for brevity and the full derivation can be provided upon request<sup>1</sup>. In brief, the method calculates noise by using a statistical model of the turbulence cross-spectrum between two points in the boundary layer (i.e. the noise source) and uses this information as an input to a Green's function solution for airfoil trailing edge far-field noise originally developed by Ffowcs-Williams and Hall (1970). A computational fluid dynamics (CFD) RANS solution is used to calculate turbulence properties about the trailing edge. This information is used to estimate the turbulence cross spectrum, which is then converted to noise via a summation procedure.

The equations of the model are summarised below.

### Noise Estimation

The model will provide the far-field acoustic auto-spectrum at a point  $\mathbf{x}$  from the trailing edge as a function of frequency  $\omega$  (i.e.  $S(\mathbf{x}, \omega)$ ),

$$S(\mathbf{x}, \omega) = \sum_{V(\mathbf{y}_1)} \sum_{V(\mathbf{y}_2)} \mathcal{Y}[u_r^{*}(\mathbf{y}_1)\hat{u}_r^{*}(\mathbf{y}_2)]F(\mathbf{y}_1)F(\mathbf{y}_2)dV(\mathbf{y}_2)dV(\mathbf{y}_1) \quad (1)$$

$$\mathcal{Y} = \frac{\rho_0^2 \omega \sin \phi \cos^2 \frac{\theta}{2}}{8\pi^3 c r_o(\mathbf{y}_1)^{3/2} r_o(\mathbf{y}_2)^{3/2} R(\mathbf{y}_1)R(\mathbf{y}_2)} \quad (2)$$

where  $\omega$  is the angular frequency,  $\rho_0$  is the undisturbed fluid density,  $V$  is the volume of fluid considered in the noise summation,  $\theta$  is the angle of the observer with respect to the trailing edge plane,  $c$  is the speed of sound,  $r_o$  is the distance of the element of fluid to the trailing edge,  $R$  is the distance from the observer to the element of fluid,  $\mathbf{y}$  is the position of the element of fluid and subscripts, 1 and 2 refer to the two fluid elements used in each summation step. In this paper, the general notation is defined:  $w^*$  is the Fourier transform of  $w$ .

The function  $F$  is a mean flow function,

$$F(\mathbf{y}) = \left\{ (\bar{U}_r - f_a \bar{U}_\theta) \cos \frac{1}{2} \theta_0 - (\bar{U}_r + f_a \bar{U}_\theta) \sin \frac{1}{2} \theta_0 \right\} \quad (3)$$

where the overbar denotes time-averaged mean, the prime is the fluctuating component of the velocity (so that  $u = \bar{U} + u'$ ) and  $\theta_0$  is the angle a turbulent eddy makes with the trailing edge. The fluctuating velocity components can be related to each other using an anisotropy factor  $f_a$ ,

$$u_r^{*} = f_a u_\theta^{*} \quad (4)$$

for an isotropic flow,  $f_a = 1$ . The subscript  $r$  refers to the radial component and  $\theta$  the tangential component with respect to the trailing edge.

Using the information contained in the RANS solution grid, the double sum can be evaluated. The remaining item to be defined is the velocity cross spectrum  $u_r^{*}(\mathbf{y}_1)\hat{u}_r^{*}(\mathbf{y}_2)$ . This is, in fact, the cross-spectral density,

$$u_r^{*}(\mathbf{y}_1)\hat{u}_r^{*}(\mathbf{y}_2) = \Phi(\mathbf{y}_1, \mathbf{y}_2, \omega) \quad (5)$$

### Turbulence Cross Spectrum

The cross spectrum model is based on a Gaussian formulation of the two-point space-time correlation function (also used by Morris and Farassat (2002) for jet noise predictions),

$$R_m(\mathbf{y}_1, \boldsymbol{\xi}, \tau) = Au_s^2 \exp\left(-\frac{|\boldsymbol{\xi}|^2}{\ell_s^2} - \omega_s^2 \tau^2\right) \quad (6)$$

where  $\ell_s$  is a characteristic length scale,  $\omega_s$  is a characteristic frequency in the moving frame,  $u_s$  is a velocity scale that characterises the velocity fluctuations and  $A$  is a scalar value that determines the magnitude of the correlation.

Converting to a cross spectrum we have,

$$\Phi(\mathbf{y}_1, \boldsymbol{\xi}, \omega) = \frac{A\sqrt{\pi}}{\omega_s} u_s^2 \exp\left(-\frac{|\boldsymbol{\xi}|^2}{\ell_s^2}\right) \exp\left(-\frac{\omega^2(1-M_c)^2}{4\omega_s^2}\right) \quad (7)$$

<sup>1</sup>The full derivation will appear in a major journal publication in the near future. A manuscript showing the derivation can be downloaded here : <http://www.mecheng.adelaide.edu.au/~cdoolan/Papers/Theory1.pdf>

where,

$$\xi = y_2 - y_1 \quad (8)$$

To link this model to a CFD solution (i.e. RANS calculated turbulence data), the following is used,

$$u_s = \sqrt{2k/3}, \quad \omega_s = 2\pi/\tau_s, \quad \tau_s = c_\tau k/\varepsilon, \quad \ell_s = c_\ell k^{3/2}/\varepsilon \quad (9)$$

where  $k$  is the turbulent kinetic energy,  $\varepsilon$  is the turbulent dissipation and  $c_\tau$  and  $c_\ell$  are constants that will be determined below.

## FLOW MODEL

The required mean turbulence data ( $k$  and  $\varepsilon$ ) are calculated using a CFD solution of the turbulent flow field about the trailing edge. In this work, the OpenFOAM (Weller et al. 1998) code is used for this purpose. Turbulence closure is provided by the standard  $k - \varepsilon$  model (Launder and Spalding 1972), the RNG  $k - \varepsilon$  model (Yakhot and Speziale 1992), the  $k - \omega$  model (Wilcox 1988) and the SST  $k - \omega$  model (Menter 1992).

The RANS equations are discretised using a structured finite-volume method within the OpenFOAM software package. The convective and diffusive terms are evaluated using a second-order accurate upwind method for the  $k - \varepsilon$  model and a first order accurate upwind method for all other models. The Semi-Implicit Method for Pressure-Linked Equations (SIMPLE) algorithm (Ferziger and Perić 1999) was used as an implicit solution scheme with a solution tolerance of  $10^{-6}$ .

## RESULTS

### Test Case: Sharp Edged Flat Plate

A sharp edged flat plate is considered as a test case for RSNM. Figure 1 shows a schematic of the test case. Air passes over a flat plate from the left to the right with freestream velocity  $U_\infty$ , generating a turbulent boundary layer on its top surface. Flow unsteadiness (turbulence) exists between the boundary layer edge and the flat plate wall (i.e. in the boundary layer). When this turbulent flow is convected past the sharp edge, the acoustic source characteristics close to the edge (those within approximately one wavelength) are modified so that they become more efficient (Ffowcs-Williams and Hall 1970). This results in strong broadband acoustic radiation to the far-field.

The sharp edged flat plate has been chosen as a test case because accurate flow and acoustic validation data are available for model development. The test case has a Reynolds number of  $Re = U_\infty L/\nu = 5.5 \times 10^5$  (based on the plate length,  $L$  and kinematic viscosity,  $\nu$ ) and  $Re_\theta = 1410$  (based on the boundary layer momentum thickness  $\theta$ , a measure of the momentum loss due to viscous stresses in the boundary layer, see Schlichting et al. (2000)). These are identical flow conditions as the direct numerical simulation (DNS) of Spalart (1988), who provides a database of boundary layer turbulence quantities. A DNS study is one of the most accurate means of obtaining unsteady fluid flow information, as no assumptions are made in the solution of the Navier Stokes equations. DNS has been shown to have excellent comparison with experiments (e.g. Eggels et al. (2006)), however is limited to low Reynolds numbers due to its high computational cost.

Semi-empirical trailing edge noise models use the assumption of chordwise and spanwise turbulence homogeneity in their

derivation (Howe 1978). As the sharp edged flat plate is the closest approximation to this in nature, semi-empirical models will provide an accurate noise estimate for validation purposes. Here, the semi-empirical model of Howe (1978) is used. This semi-empirical model needs an estimate of the turbulent wall pressure spectrum and the flat plate, zero-pressure-gradient model of Willmarth and Roos (1965) is used for this purpose.

## Flow Results

### Grid Refinement Study

Parameter	Inlet	Outlet	Fixed Wall
$U/U_\infty$	1	Zero gradient	0
$k/U_\infty^2$	0.015	Zero gradient	0
$\varepsilon U_\infty^3/L$	11.15	Zero gradient	0
$P/P_\infty$	Zero gradient	0	Zero gradient

Table 1: Boundary conditions

The grid used for this study is a structured grid composed of two blocks (see Figure 2); block number 1 had an initial resolution of  $300 \times 30$  cells, which was increased by a factor of 1.2 in each refinement step of the grid refinement study. Block number 2 had an initial resolution of  $30 \times 10$  cells, and mesh grading was used to gradually decrease resolution as distance from the wall increases. The resolution of block number 2 was increased by the same factor as block 1 in the  $x$  direction and kept constant in the  $y$  direction at 10 cells throughout the grid refinement study. A wall function Wilcox (2006) was used for the near wall region, and an inflow turbulence of 0.1% was assumed. This level of turbulence is similar to that obtained in many aeroacoustic facilities (Doolan and Leclercq 2007). Free stream velocity and chord length were defined as unity, and kinematic viscosity was defined as  $\nu = 1.8149 \times 10^{-6}$  to obtain a Reynolds number of  $Re = U_\infty L/\nu = 5.5 \times 10^5$  at the trailing edge. Table 1 shows a summary of the boundary conditions used in the RANS simulations. The initial condition of *zero gradient* means the gradient normal to the boundary is zero.

The parameters chosen for the grid refinement study were the momentum thickness  $\theta$  and displacement thickness  $\delta^*$  (a measure of the mass flow rate loss due to viscous stresses in the boundary layer, Schlichting et al. (2000)). The grid resolution was increased until  $\theta$  and  $\delta^*$  converged. The results are independent of grid resolution beyond 18920 cells, so the 27560 cell mesh was chosen for acoustic calculations. Table 2 shows a summary of the grid refinement study.

Model	N <sup>o</sup> of Cells	y+	$\delta^*/L$	$\theta/L$
$k - \varepsilon$	975	21.87	0.0032	0.0022
$k - \varepsilon$	13320	17.79	0.0034	0.0023
$k - \varepsilon$	18920	14.91	0.0035	0.0023
$k - \varepsilon$	27560	12.50	0.0035	0.0023
RNG $k - \varepsilon$	975	20.92	0.0033	0.0022
RNG $k - \varepsilon$	13320	17.40	0.0034	0.0023
RNG $k - \varepsilon$	18920	14.63	0.0035	0.0022
RNG $k - \varepsilon$	27560	12.24	0.0035	0.0022
$k - \omega$	975	21.58	0.0034	0.0023
$k - \omega$	975	17.90	0.0035	0.0024
$k - \omega$	975	15.41	0.0035	0.0024
$k - \omega$	975	12.62	0.0035	0.0024
SST $k - \omega$	975	21.37	0.0033	0.0023
SST $k - \omega$	975	17.79	0.0034	0.0023
SST $k - \omega$	975	14.95	0.0035	0.0023
SST $k - \omega$	975	12.47	0.0035	0.0023

Table 2: Grid refinement study.

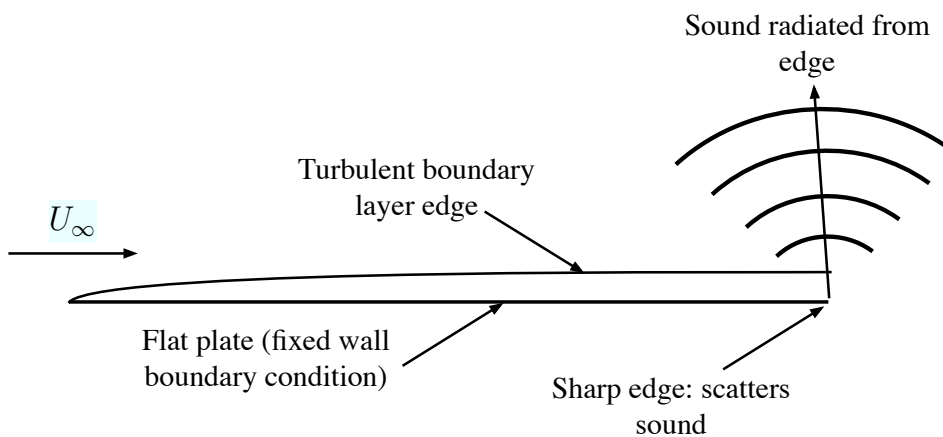


Figure 1: Schematic of a boundary layer developing over a sharp edged flat plate

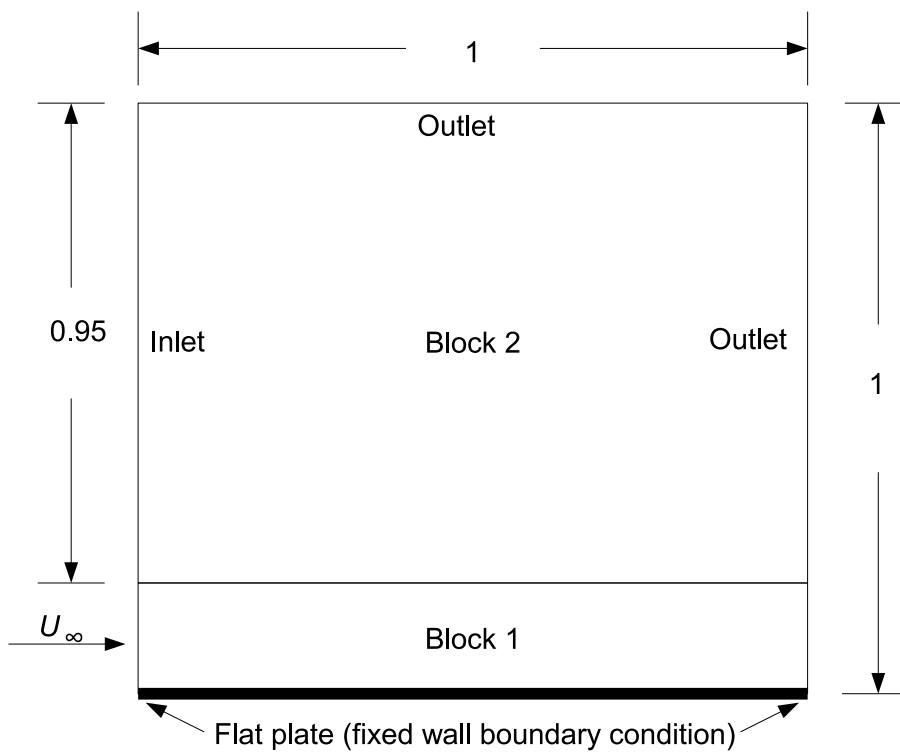


Figure 2: Schematic of the domain and grid used for RANS simulations.

### Comparison with DNS data

Figure 3 shows the mean velocity profile in the boundary layer, normalised by the free stream velocity ( $U_\infty$ ) and plotted against distance to the wall normalised by the boundary layer thickness  $\delta$ . Good agreement is observed for all models when compared to the DNS of Spalart (1988). Figure 4 shows the turbulent kinetic energy profile for all turbulence models, normalised by the squared of the friction velocity  $u_\tau^2 = \tau_w/\rho$ , where  $\tau_w$  is the wall shear stress. Comparison with the turbulent kinetic energy DNS data of Spalart (1988) is not as good as for the mean velocity profile, however it is nearly identical to the profiles obtained in similar validation work (Yang and Shih 1993).

The rate of dissipation of turbulent kinetic energy is plotted in figure 5 as a function of non-dimensional distance to the wall (normalised by  $\delta$ ). All models produce a similar profile.

### Acoustic Results

This section will discuss the acoustic results obtained using RSNM. After a grid refinement study, the RANS turbulence data presented above are used as an input to RSNM to obtain noise spectra. The performance of the RSNM is assessed by comparing the predicted noise spectra to the semi-empirical model of Howe (1978) for an observer positioned at a distance of 1.5 chord lengths directly over the trailing edge (at a 90 degree angle to the freestream).

#### Grid refinement Study

A grid refinement study was conducted to determine the resolution required to obtain a grid independent solution. The data were sampled over a domain extending from the trailing edge to one  $\delta$  upstream of the trailing edge, and one  $\delta$  in the vertical direction. Grid resolution was doubled in each refinement step until convergence was achieved. The parameters used in the model for this study were:  $c_\ell = 1$ ,  $c_t = 1.2$  and  $A = 10^{-2}$ . Figure 6 shows that a resolution of  $40 \times 40$  cells is sufficient. To determine the required extent of the domain in the upstream direction, the domain was extended in successive steps of one  $\delta$  in the upstream direction with the resolution determined in the grid refinement study (1600 cells per  $\delta^2$ ). Figure 7 shows that extending the domain beyond two  $\delta$  upstream of the trailing edge has no effect on the resulting spectra. Note that data were not sampled in the wake, downstream of the trailing edge. This might be an important component of the trailing edge noise source and will be studied during the next phase of RSNM development.

#### Comparison with Semi-Empirical Noise Model

In this section, the power spectral density calculated using RSNM is compared with the semi-empirical model of Howe (1978). Results are presented using two sets of parameters (constants  $A$ ,  $c_\ell$ ,  $c_t$ ), a low frequency set and a high frequency set, which have been found to provide a good match with the semi-empirical model of Howe (1978) at frequencies below 2000 Hz and above 2000 Hz respectively.

Figure 8 compares the calculated power spectral density with the semi-empirical model of Howe (1978). The parameters used were  $c_\ell = 10^{-5}$ ,  $c_t = 10$  and  $A = 0.6$ . The agreement between RSNM and the semi-empirical model of Howe (1978) is excellent for frequencies below 2000 Hz. Similarly, figure 9 shows the predicted spectra using the high frequency parameters ( $c_\ell = 1$ ,  $c_t = 1.2$  and  $A = 10^{-2}$ ). Excellent agreement is observed for frequencies above 2000 Hz. For both frequency ranges, no significant difference is observed between the predictions made using different turbulence models. This is explained by the similarity of the RANS results produced by all

turbulence models.

### CONCLUSION

A new method (RSNM) for predicting trailing edge noise based on a RANS solution has been presented and applied to a flat plate test case. It shows good agreement with the empirical model of Howe (1978). The RSNM has three parameters that are found by best fit to experimental data. Two sets of parameters are needed, one for frequencies below 2000 Hz and one for frequencies above 2000 Hz. Four turbulence models were used to provide the required flow data; the results indicate that the choice of turbulence model has no significant effect on the resulting spectra. The method is promising as a tool for engineering design, as it can give accurate results with very modest computational requirements. A sampling domain of two boundary layer heights in the  $x$ -wise direction with a resolution of 40 cells per boundary layer height upstream from the trailing edge was shown to be sufficient to obtain grid independent results.

Future work will focus on the application of RSNM to more challenging geometries such as real airfoils and the development of new turbulent velocity cross spectrum models. More appropriate velocity cross spectrum models will eliminate the need for frequency dependent parameters.

### REFERENCES

- W. K. Blake. *Mechanics of flow-induced sound and vibration*, volume 2. Academic Press, New York, 1986.
- KL Chandiramani. Diffraction of evanescent waves, with applications to aerodynamically scattered sound and radiation from un baffled plates. *The Journal of the Acoustical Society of America*, 55, 1974.
- C.J. Doolan and D. Leclercq. An anechoic wind tunnel for the investigation of the main-rotor/tail-rotor blade vortex interaction. In *Proceedings of the 6th Australian Vertiflite Conference on Helicopter Technology*. American Helicopter Society International, Inc., March 2007.
- JGM Eggels, F. Unger, MH Weiss, J. Westerweel, RJ Adrian, R. Friedrich, and FTM Nieuwstadt. Fully developed turbulent pipe flow: a comparison between direct numerical simulation and experiment. *Journal of Fluid Mechanics*, 268:175–210, 2006.
- R Ewert. Broadband slat noise prediction based on caa and stochastic sound sources from a fast random particle-mesh (rpm) method. *Computers and Fluids*, 37(4):369–387, Jan 2008. doi: 10.1016/j.compfluid.2007.02.003.
- R Ewert, C Appel, J Dierke, and M Herr. Rans/caa based prediction of naca 0012 broadband trailing edge noise and experimental validation. *15th AIAA/CEAS Aeroacoustics Conference, AIAA-2009-3269*, May 2009.
- J.H. Ferziger and M. Perić. *Computational methods for fluid dynamics*. Springer Berlin, 1999.
- JE Ffowcs-Williams and LH Hall. Aerodynamic sound generation by turbulent flow in the vicinity of a scattering half plane. *Journal of Fluid Mechanics*, 40(4):657–670, 1970.
- S Glegg, B Morin, O Atassi, and R Reba. Using rans calculations of turbulent kinetic energy to provide predictions of trailing edge noise. *14th AIAA/CEAS Aeroacoustics Conference (29th AIAA Aeroacoustics Conference) 5 - 7 May 2008, Vancouver, British Columbia Canada, AIAA 2008-2993*, May 2008.
- X Gloerfelt and Thomas Le Garrec. Trailing edge noise from an isolated airfoil at a high reynolds number. *15th AIAA/CEAS Aeroacoustics Conference, AIAA-2009-3201*, pages 1–26, May 2009.
- M. S Howe. A review of the theory of trailing edge noise. *Journal of Sound and Vibration*, 61:437, Dec 1978.

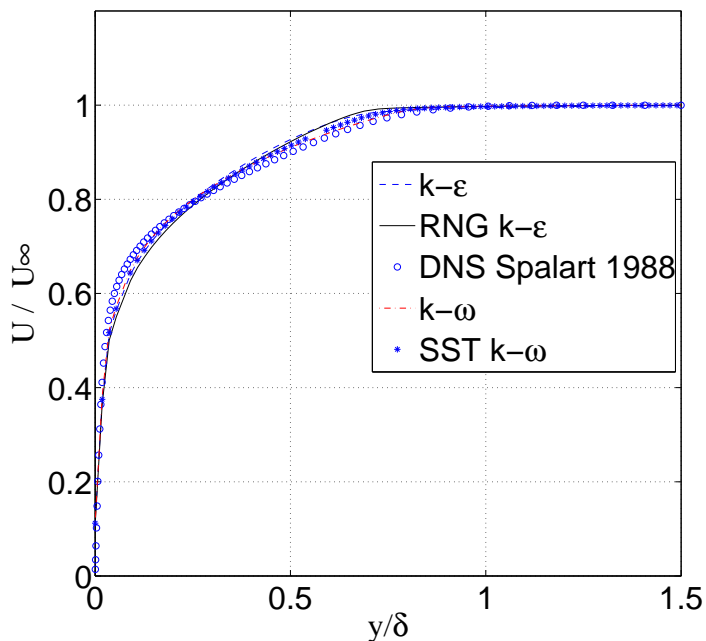


Figure 3: Mean velocity profiles at the trailing edge for all turbulence models, plotted against the DNS data of Spalart (1988).

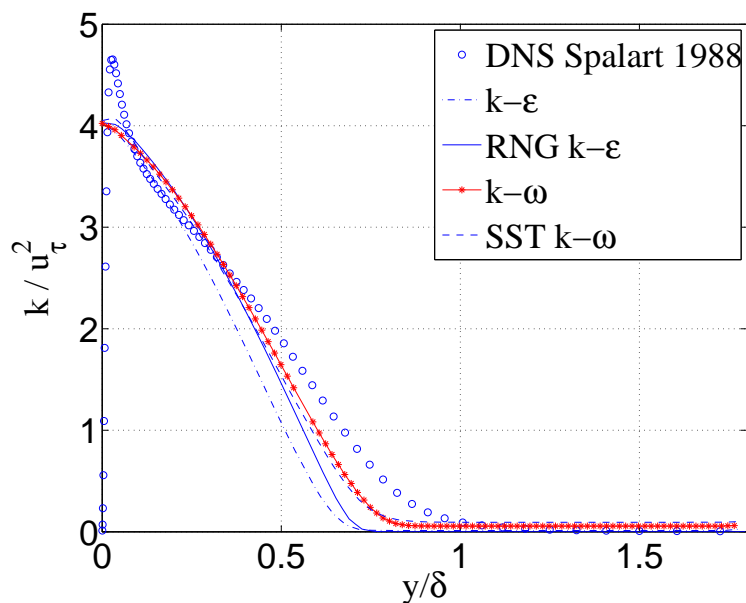


Figure 4: Turbulent kinetic energy profiles at the trailing edge calculated using all turbulence models, plotted against the DNS data of Spalart (1988).

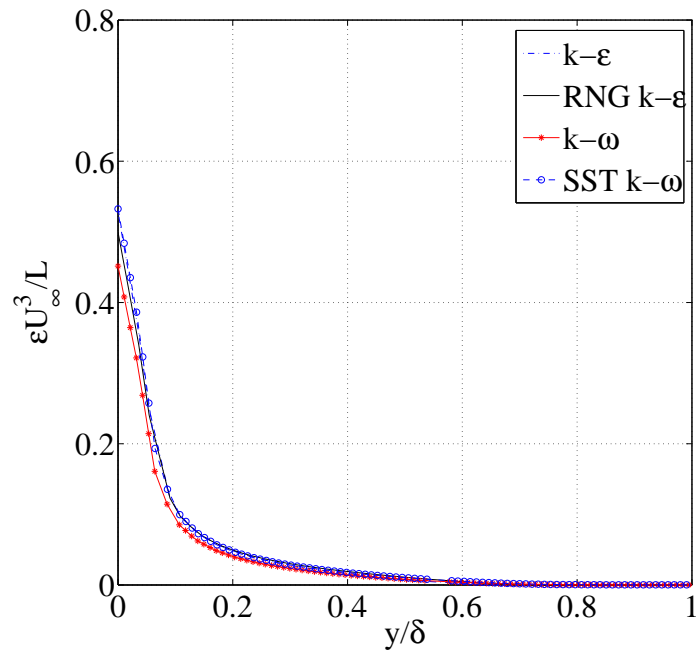


Figure 5: Rate of dissipation of turbulent kinetic energy per unit mass ( $\epsilon$ ) at the trailing edge for all turbulence models.

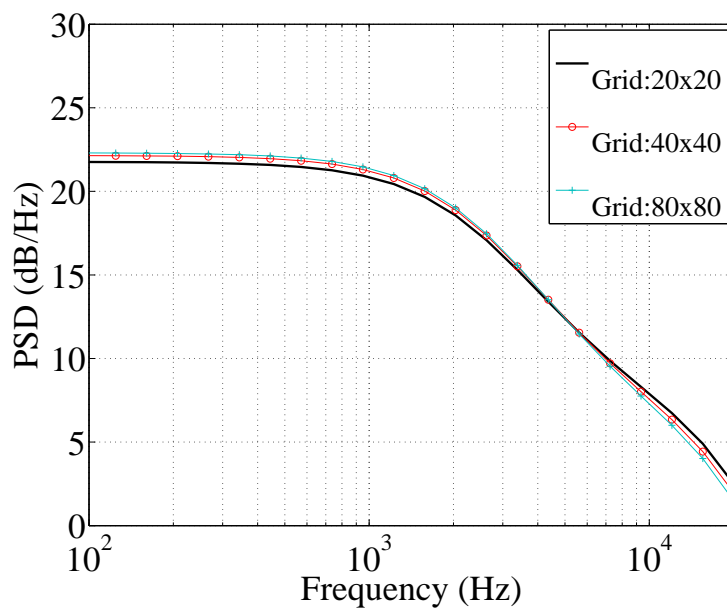


Figure 6: Power spectral density calculated using RSNM with RNG  $k - \epsilon$  turbulence model, for different acoustic grid resolutions sampling up to one boundary layer height  $\delta$  upstream from the trailing edge.

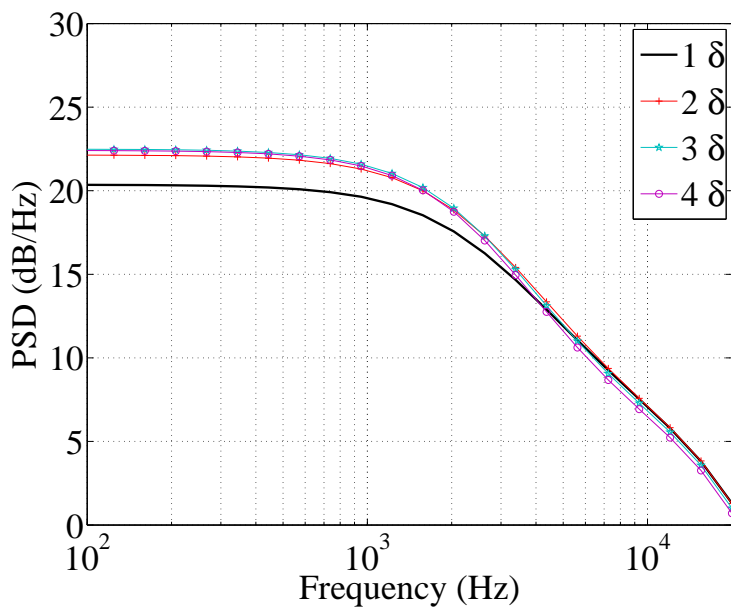


Figure 7: Power spectral density calculated using RSNM with RNG  $k - \epsilon$  turbulence model, for four different domain sizes.

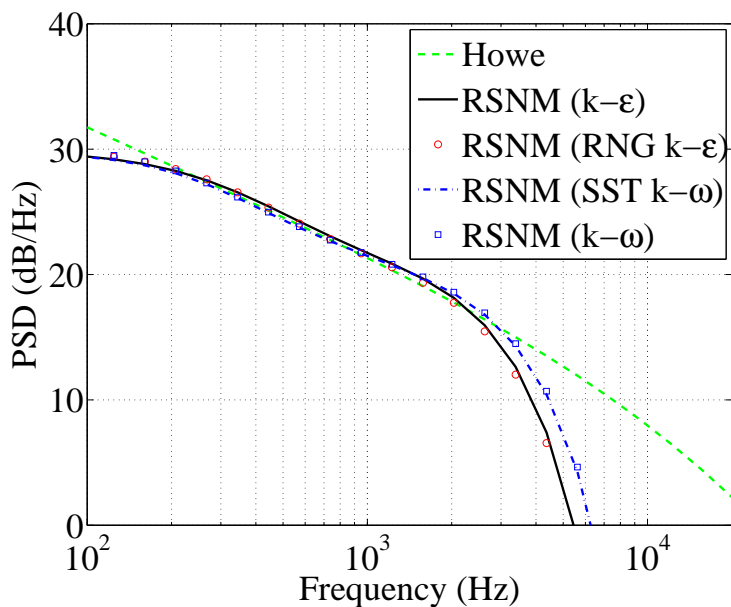


Figure 8: Power spectral density calculated using RSNM with the low frequency parameters ( $A = 0.6, c_\ell = 10^{-5}, c_\tau = 10$ ) for all turbulence models, plotted against the empirical model of Howe (1978).

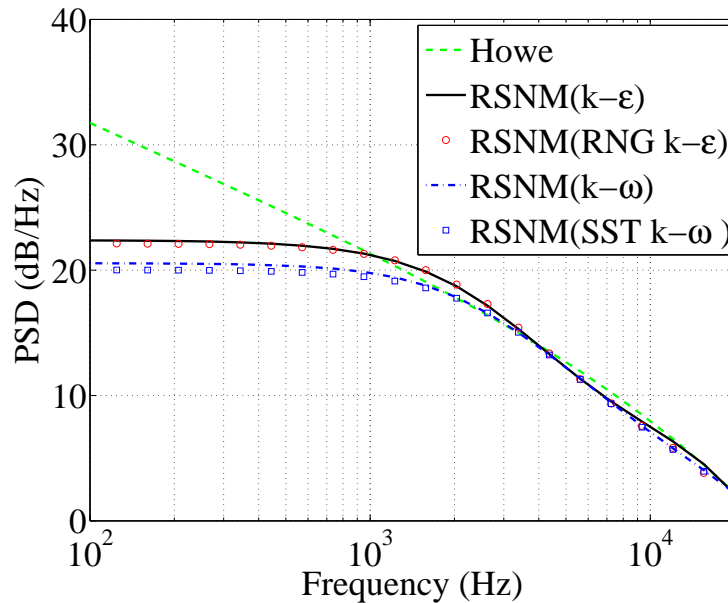


Figure 9: Power spectral density calculated using RSNM with the high frequency parameters ( $A = 10^{-2}$ ,  $c_l = 1$ ,  $c_\tau = 1.2$ ) for all turbulence models, plotted against the empirical model of Howe (1978).

R. F. Jones, C. J. Doolan, and M. D. Teubner. Stochastically generated turbulence for wall stochastically generated turbulence for wall bounded flows. *ANZIAM Journal*, under review, 2010.

M Kamruzzaman, Th Lutz, A Herrig, and E Kramer. Rans based prediction of airfoil trailing edge far-field noise: Impact of isotropic & anisotropic turbulence. *14th AIAA/CEAS Aeroacoustics Conference (29th AIAA Aeroacoustics Conference) 5 - 7 May 2008, Vancouver, British Columbia Canada, AIAA 2008-2867*, May 2008.

B. E. Launder and D. B. Spalding. The Numerical Computation of Turbulent Flows. *Comput. Methods Appl. Mech. Eng.*, 4:269–289, 1972.

T. Lutz, A. Herrig, W. Wurz, M. Kamruzzaman, and E. Kramer. Design and wind-tunnel verification of low-noise airfoils for wind turbines. *AIAA Journal*, 45(4):779–785, Apr 2007.

E. Manoha, B. Troff, and P. Sagaut. Trailing-edge noise prediction using large-eddy simulation and acoustic analogy. *AIAA Journal*, 38(4):575–583, 2000.

Alison L Marsden, Meng Wang, J. E Dennis, and Parviz Moin. Trailing-edge noise reduction using derivative-free optimization and large-eddy simulation. *Journal of Fluid Mechanics*, 572:13–36, 2007. doi: 10.1017/S0022112006003235.

F. R. Menter. Improved Two-Equation  $k - \omega$  Turbulence models for Aerodynamic Flows, NASA Ames, CA. *NASA Technical Memorandum TM-103975*, 1992.

PJ Morris and F Farassat. Acoustic analogy and alternative theories for jet noise prediction. *AIAA Journal*, 40(4):671–680, Jan 2002.

P.M.C. Morse and K.U. Ingard. *Theoretical acoustics*. Princeton Univ Pr, 1986.

R Sandberg and N Sandham. Direct numerical simulation of turbulent flow past a trailing edge and the associated noise generation. *Journal of Fluid Mechanics*, 596:353–385, 2008.

H. Schlichting, K. Gersten, and K. Gersten. *Boundary-layer theory*. Springer Verlag, 2000.

P.R. Spalart. Direct simulation of a turbulent boundary-layer up to  $r\text{-}\theta=1410$ . *Journal of Fluid Mechanics*, 187:61–98, Jan 1988.

N Spitz. Prediction of trailing edge noise from two-point velocity correlations. *Masters Thesis, Virginia Tech.*, Jan 2005. URL <http://scholar.lib.vt.edu/theses/available/etd-05122005>

CKW Tam and L Auriault. Jet mixing noise from fine-scale turbulence. *AIAA Journal*, 37(2):145–153, Jan 1999.

H.G. Weller, G. Tabor, H. Jasak, and C. Fureby. A tensorial approach to cfd using object orientated techniques. *Computers in Physics*, 12(6):620–631, 1998.

D. C. Wilcox. Reassessment of the Scale-determining Equation for Advanced Turbulence Models. *AIAA*, 26:1299–1310, 1988.

D.C. Wilcox. *Turbulence Modeling for CFD*. DCW Industries, La Canada, CA, USA, 3rd edition, 2006.

WW Willmarth and FW Roos. Resolution and structure of the wall pressure field beneath a turbulent boundary layer. *Journal of Fluid Mechanics*, 22:81–94, 1965.

J Winkler, S Moreau, and Thomas Carolus. Large-eddy simulation and trailing-edge noise prediction of an airfoil with boundary-layer tripping. *15th AIAA/CEAS Aeroacoustics Conference, AIAA-2009-3197*, May 2009.

Orszag S. A. Thangam S. Gatski T. B. Yakhot, V. and C. G. Speziale. Development of Turbulence Models for Shear Flows by a Double Expansion Technique. *Phys. Fluids A*, 4(7):1510–1520, 1992.

Z. Yang and TH Shih. New Time Scale Based k-epsilon Model for Near-Wall Turbulence. *AIAA Journal*, 31(7), 1993.